

## Segregation and precipitation of Er in Ge

S. O. Kucheyev<sup>a)</sup>

Lawrence Livermore National Laboratory, Livermore, California 94551

J. E. Bradby, S. Ruffell, and C. P. Li

Department of Electronic Materials Engineering, The Australian National University, Canberra, ACT 0200, Australia

T. E. Felter and A. V. Hamza

Lawrence Livermore National Laboratory, Livermore, California 94551

(Received 14 December 2006; accepted 2 May 2007; published online 29 May 2007)

Although Er-doped Ge nanomaterials are attractive for photonic applications, very little is known about the basic properties of Er in Ge. Here, the authors study the annealing behavior of Ge implanted with keV Er ions to doses resulting in  $\lesssim 1$  at. % of Er. Large redistribution of Er, with segregation at the amorphous/crystalline interface, starts at  $\geq 500$  °C, while lower temperatures are required for material recrystallization. However, even at 400 °C, Er forms precipitates. The concentration of Er trapped in the bulk after recrystallization decreases with increasing temperature but is independent of the initial bulk Er concentration for the range of ion doses studied here.

© 2007 American Institute of Physics. [DOI: 10.1063/1.2743881]

The behavior of Er in Si has been extensively studied for the past decade, stimulated by the drive for integration of photonics and Si technology.<sup>1</sup> In contrast, only a few previous studies have focused on the Ge:Er system.<sup>2–6</sup> Such a considerably smaller interest in Ge:Er is due to a very modest role of Ge in microelectronics and the fact that the band gap of bulk Ge (0.67 eV at 20 °C) is smaller than the Er-related emission of interest in communication technologies ( $\sim 1.5$   $\mu\text{m}$  or  $\sim 0.8$  eV).

It has been demonstrated that, with decreasing size of Ge nanoparticles below a few nanometers, their band gap rapidly increases.<sup>7</sup> The number of studies of Ge-based nanomaterials, including nanoparticles, nanowires, and nanofoams, is currently growing fast since nanostructured Ge exhibits some advantages over Si. These include stronger quantum confinement effects and better controlled oxidation.<sup>7</sup> In addition, Ge is known to spontaneously develop nanoporosity during ion bombardment under certain irradiation conditions, which could be exploited for the fabrication of novel nanodevices.<sup>8</sup>

Although Er-doped Ge nanostructures have been a subject of previous reports,<sup>2–4</sup> we are not aware of any studies of the basic properties of Er in Ge, such as diffusivity, solubility, and segregation. Since this information is crucial for the development of Ge:Er-based devices,<sup>9</sup> in this letter, we study the behavior of Er-implanted Ge during annealing with thermal budgets needed for the recovery of crystallinity in a disordered Ge lattice. Our results show that crystallinity is conveniently recovered at temperatures ( $\sim 400$  °C) below the onset of significant redistribution of Er, starting at  $\sim 500$  °C. This is an advantage over the Si:Er system, where recrystallization (without codoping with light elements such as oxygen) is accompanied by complex, concentration and temperature dependent segregation of Er at the amorphous/crystalline (*a/c*) interface.<sup>1</sup> However, Er forms precipitates in Ge even at 400 °C. Our results also show that, for temperatures  $\geq 500$  °C, Er atoms in Ge are segregated at the *a/c* interface. The concentration of Er left in the Ge bulk after

solid phase epitaxy (SPE) decreases with increasing annealing temperature but is independent of the initial bulk Er concentration for the ion doses studied here.

Single crystal (100) Ge was implanted with 500 keV Er<sup>+</sup> ions to doses of  $2.2 \times 10^{15}$  and  $4.4 \times 10^{15}$  cm<sup>-2</sup> with a beam flux  $\lesssim 2 \times 10^{11}$  cm<sup>-2</sup> s<sup>-1</sup>. During implantation, the ion beam direction was at  $\sim 7^\circ$  off the sample normal in order to minimize channeling, and the samples were kept at liquid nitrogen temperature to avoid the formation of a nanoporous structure observed during room-temperature high-dose keV-ion bombardment of Ge.<sup>8</sup> After implantation, samples were processed in a rapid thermal annealer in a nitrogen ambient at atmospheric pressure for 120 s in the temperature range of 400–800 °C.

Depth profiles of lattice disorder and Er atoms were studied by Rutherford backscattering/channeling (RBS/C) spectrometry with 2.0 MeV <sup>4</sup>He<sup>+</sup> ions incident along the [100] direction and backscattered into detectors at 112° and 164° relative to the incident beam direction. Analysis of RBS spectra was done with stopping powers and scattering cross sections from the RUMP code.<sup>10</sup> Selected specimens were studied by cross-sectional transmission electron microscopy (XTEM) with a 300 keV electron beam.

Figure 1 shows RBS/C spectra illustrating the evolution of lattice disorder upon annealing of Ge bombarded with 500 keV Er ions to a dose of  $4.4 \times 10^{15}$  cm<sup>-2</sup>. It is seen from Fig. 1 that the as-implanted sample has an  $\sim 3000$ -Å-thick surface amorphous layer. This layer recrystallizes via SPE even at the lowest annealing temperature studied (400 °C), which is consistent with previous studies showing that nominally undoped Ge recrystallizes via SPE at temperatures  $\geq 300$  °C.<sup>11</sup> The thickness of the residual surface defective layer left after SPE is a function of annealing temperature. This effect is better illustrated by the inset of Fig. 1, showing the dependence of the normalized minimum RBS/C yield on annealing temperature.

Such a complex behavior of the residual bulk damage and the thickness of the residual surface disordered layer on annealing temperature, revealed in Fig. 1, is directly related to segregation and trapping of Er during SPE. Figure 2

<sup>a)</sup>Electronic mail: kucheyev@llnl.gov

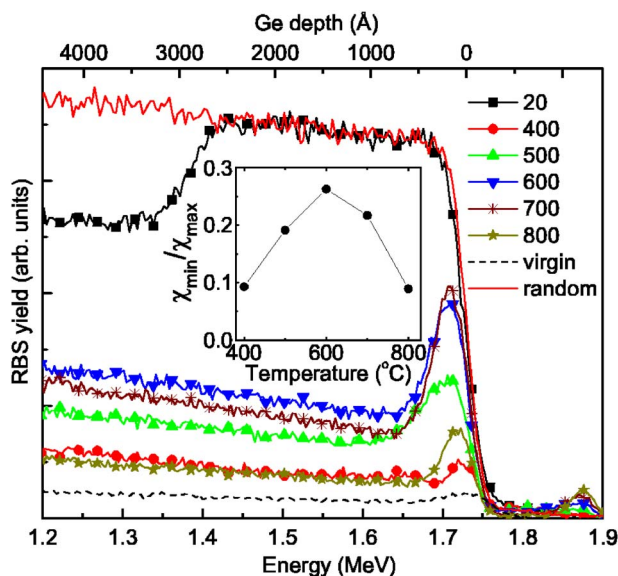


FIG. 1. (Color online) RBS/C spectra (acquired with a scattering angle of  $112^\circ$ ) showing the evolution of lattice disorder upon annealing of Ge bombarded at  $-196^\circ\text{C}$  with 500 keV Er ions to a dose of  $4.4 \times 10^{15}\text{ cm}^{-2}$ . Annealing temperatures (in  $^\circ\text{C}$ ) are indicated in the legend. For clarity, only every seventh experimental point is shown. The inset shows the annealing temperature dependence of the normalized minimum RBS/C yield.

shows XTEM images of Ge bombarded at  $-196^\circ\text{C}$  with 500 keV Er ions to a dose of  $4.4 \times 10^{15}\text{ cm}^{-2}$  and annealed at  $400^\circ\text{C}$  [Fig. 2(a)],  $500^\circ\text{C}$  [Fig. 2(b)], and  $800^\circ\text{C}$  [Fig. 2(c)].<sup>12</sup> In agreement with RBS/C results from Fig. 1, these XTEM images show that the  $\sim 3000\text{-\AA}$ -thick surface amorphous layer formed by the Er implant recrystallizes via SPE even at  $400^\circ\text{C}$ . However, such SPE is not complete, and residual surface amorphous layers are clearly visible in Figs. 2(a)–2(c). The thickness of such residual amorphous layers changes from  $\sim 250$  to  $\sim 300$  to  $\sim 120\text{ \AA}$  with increasing annealing temperature from  $400$  to  $500$  to  $800^\circ\text{C}$ , respectively. Figure 2 also reveals precipitation of Er (presumably forming Er germanates) for all the three annealing temperatures and significant Er segregation at the  $a/c$  interface for the sample annealed at  $500^\circ\text{C}$  [Fig. 2(b)]. Such extensive Er segregation at the  $a/c$  interface [Fig. 2(b)] is consistent with a broad surface peak in the RBS/C spectrum from the sample annealed at  $500^\circ\text{C}$  [Fig. 1]. High-resolution XTEM (images not shown) also shows that the crystal adjacent to the  $a/c$  interface in the sample annealed at  $800^\circ\text{C}$  [Fig. 2(c)] has twin defects. This is consistent with a different thermal evolution of implantation-produced defects at temperatures close to the melting point of Ge ( $\sim 940^\circ\text{C}$ ).

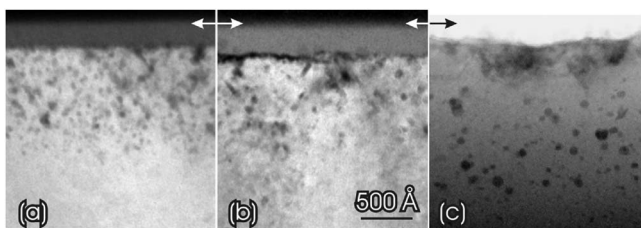


FIG. 2. Bright-field XTEM images of Ge bombarded at  $-196^\circ\text{C}$  with 500 keV Er ions to a dose of  $4.4 \times 10^{15}\text{ cm}^{-2}$  and annealed at (a)  $400^\circ\text{C}$ , (b)  $500^\circ\text{C}$ , and (c)  $800^\circ\text{C}$ . The sample surface is indicated by arrows. All images are of the same magnification.

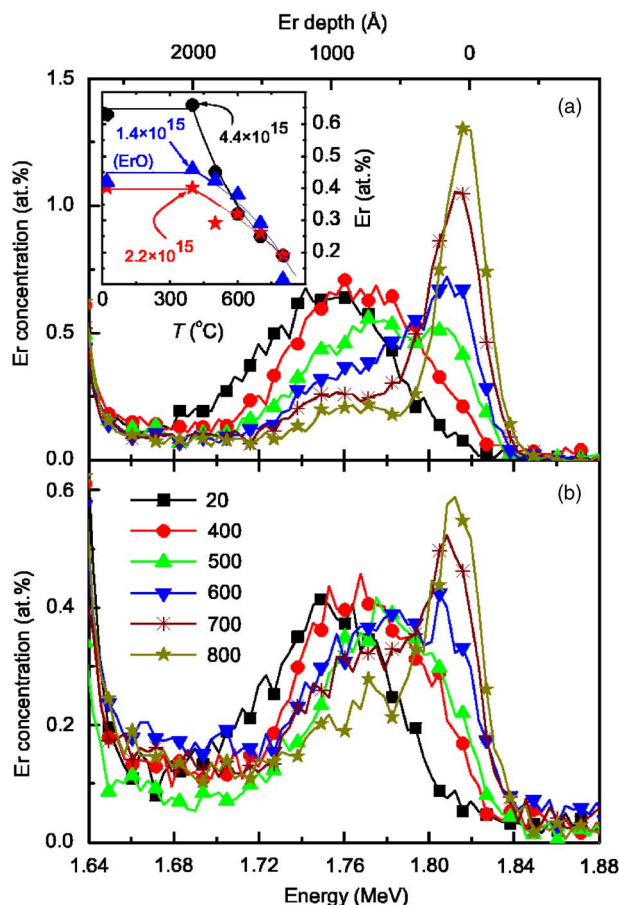


FIG. 3. (Color online) RBS spectra (acquired with a scattering angle of  $164^\circ$ ) showing the evolution of Er depth profiles upon annealing of Ge bombarded at  $-196^\circ\text{C}$  with 500 keV Er ions to doses of (a)  $4.4 \times 10^{15}$  and (b)  $2.2 \times 10^{15}\text{ cm}^{-2}$ . Annealing temperatures (in  $^\circ\text{C}$ ) are indicated in the legend. For clarity, only every third experimental point is shown. The inset in (a) shows the dependence of the Er concentration at the projected ion range depth on annealing temperature for both doses of 500 keV Er ions and for a dose of  $1.4 \times 10^{15}\text{ cm}^{-2}$  of 110 keV ErO ions, as indicated (in  $\text{cm}^{-2}$ ). The solid lines in the inset are to guide the reader's eye.

The evolution of Er in Ge during SPE is further illustrated by Fig. 3(a), showing Er depth profiles in the Ge samples from Fig. 1. It is seen from Fig. 3(a) that the Er depth profile shifts slightly toward the sample surface during annealing at  $400^\circ\text{C}$ , and significant redistribution of Er, with the formation of a bimodal Er depth profile due to Er segregation at the  $a/c$  interface, occurs only for annealing temperatures  $\geq 500^\circ\text{C}$ . After annealing at  $800^\circ\text{C}$ ,  $\sim 70\%$  of the implanted Er is segregated in the near-surface layer. Figure 3(a) also shows that the concentration of Er trapped in the Ge bulk after SPE monotonically decreases from 0.7 to 0.2 at. % with increasing annealing temperature from  $400$  to  $800^\circ\text{C}$ , respectively.

Figure 3(b) shows the evolution of Er depth profiles in Ge bombarded with 500 keV Er ions to a lower dose of  $2.2 \times 10^{15}\text{ cm}^{-2}$ . A comparison of Figs. 3(a) and 3(b) reveals a similar behavior of Er implanted to the two different doses, with significant redistribution of Er starting above  $\sim 500^\circ\text{C}$ . Hence, for the Er dose range studied here, the temperatures required for the onset of Er segregation at the  $a/c$  interface during SPE of Ge are independent of the initial Er concentration. Note that, for the Si:Er system, the Er segregation is a strong function of the initial Er concentration.<sup>1</sup> Moreover, Fig. 3 shows that the concentration of Er trapped in the Ge

bulk after SPE is independent of ion dose and monotonically decreases with increasing annealing temperature. This effect is better illustrated in the inset of Fig. 3(a), showing the Er concentration at a depth of 1000 Å (corresponding to the projected range for 500 keV Er ions) as a function of annealing temperature for both ion doses.

The inset of Fig. 3(a) also shows the annealing temperature dependence of the Er concentration at the projected range depth of Er ions in Ge bombarded at  $-196\text{ }^{\circ}\text{C}$  with 110 keV ErO<sup>-</sup> cluster ions to a dose of  $1.4 \times 10^{15}\text{ cm}^{-2}$  with a beam flux of  $\approx 2 \times 10^{11}\text{ cm}^{-2}\text{ s}^{-1}$ .<sup>13,14</sup> Such Er depth profiles for 110 keV ErO cluster ion bombardment were obtained from 2 MeV <sup>4</sup>He<sup>+</sup> ion RBS analysis with a scattering angle of 101°. It is seen that the evolution of Er in ErO-implanted Ge is similar to that in Er-implanted Ge, indicating a minor effect of O impurities on the evolution of Er in Ge. This observation is in contrast to the strong effects of O on the diffusion of Er in Si.<sup>1</sup>

We also note that, for all the samples studied, the Er-related signal in RBS/C spectra was independent of whether the spectra were acquired in the [100] channeling or random direction. This indicates that Er does not reside in either substitutional or tetrahedral interstitial sites in the cubic Ge lattice. Similar results were reported in RBS/C studies of Si:Er,<sup>1</sup> while Er in Si<sub>1-x</sub>Ge<sub>x</sub> ( $x=0.1-0.8$ ) alloys has been found to prefer regular lattice sites, with specific lattice positions being strongly dependent on alloy composition.<sup>15</sup>

Finally, Fig. 3 reveals that the amount of Er segregated at the *a/c* interface during SPE increases with increasing temperature. Both increase and decrease in segregation of impurities at the surface after SPE have previously been observed in Si for different dopants.<sup>16</sup> In general, it is difficult to predict the temperature behavior of the *nonequilibrium* segregation coefficient during SPE since, in the solute trapping regime, it depends on the temperature dependencies of (i) the equilibrium segregation coefficient, (ii) diffusivity of Er at the *a/c* interface, (iii) velocity of recrystallization, and (iv) the free energy driving the phase transformation. These values are also concentration dependent. According to models of Aziz *et al.*<sup>17</sup> and Jackson *et al.*<sup>18</sup> (in the limit of small concentrations), results from Fig. 3 could be interpreted very differently, suggesting that the interface diffusivity of Er increases with temperature either more rapidly or more slowly than the regrowth velocity. Hence, further studies are currently needed to clarify the underlying physical mechanisms of the temperature dependence of nonequilibrium impurity segregation in semiconductors.

In conclusion, we have demonstrated that Er at concentrations of  $\sim 1$  at. % strongly affects the recrystallization behavior of amorphous Ge. At such concentrations, Er forms precipitates in the bulk even at 400 °C,<sup>19</sup> with significant Er segregation at the amorphous/crystalline interface starting at temperatures  $\geq 500\text{ }^{\circ}\text{C}$ . The concentration of Er trapped in the bulk after planar recrystallization of amorphous Ge decreases with increasing temperature but is independent of the initial bulk Er concentration for the range of ion doses studied here. These findings on the basic behavior of Er in Ge are important for understanding properties of Er-doped Ge nanostructures.

Work at LLNL was performed under the auspices of the U.S. DOE by the University of California, LLNL under Con-

tract No. W-7405-Eng-48. Work at the ANU was supported by the ARC.

<sup>1</sup>See, for example, reviews by A. Polman, *J. Appl. Phys.* **82**, 1 (1997); A. J. Kenyon, *Semicond. Sci. Technol.* **20**, R65 (2005).

<sup>2</sup>J. H. Chen, D. Pang, H. M. Cheong, P. Wickboldt, and W. Paul, *Appl. Phys. Lett.* **67**, 2182 (1995).

<sup>3</sup>J. Wu, P. Panchaipetch, R. M. Wallace, and J. L. Coffey, *Adv. Mater. (Weinheim, Ger.)* **16**, 1444 (2004).

<sup>4</sup>C. L. Heng, T. G. Finstad, P. P. Storas, Y. J. Li, A. E. Gunnaes, and O. Nilsen, *Appl. Phys. Lett.* **85**, 4475 (2004).

<sup>5</sup>H. Navarro, T. Timusk, W. R. Datars, and D. C. Houghton, *Appl. Phys. A: Solids Surf.* **53**, 373 (1994).

<sup>6</sup>S. L. Liew, B. Balakrishnan, S. Y. Chow, M. Y. Lai, W. D. Wnag, K. Y. Lee, C. S. Ho, T. Osipowicz, and D. Z. Chi, *Thin Solid Films* **504**, 81 (2006).

<sup>7</sup>See, for example, C. Bostedt, T. van Buuren, T. M. Willey, N. Franco, L. J. Terminello, C. Heske, and T. Moeller, *Appl. Phys. Lett.* **84**, 4056 (2004); M. Jing, M. Ni, W. Song, J. Lu, Z. Gao, L. Lai, W. N. Mei, D. Yu, H. Ye, and L. Wang, *J. Phys. Chem.* **110**, 18332 (2006).

<sup>8</sup>See, for example, I. H. Wilson, *J. Appl. Phys.* **53**, 1698 (1982); B. R. Appleton, O. W. Holland, J. Narayan, O. E. Schow III, J. S. Williams, K. T. Short, and E. Lawson, *Appl. Phys. Lett.* **41**, 711 (1982); L. M. Wang and B. C. Birtcher, *Philos. Mag. A* **64**, 1209 (1991).

<sup>9</sup>In particular, understanding behavior of Er during thermal processing of Ge is essential in our current studies of controllable Er doping of Ge nanostructures made by sequential implantation of bulk Ge with (i) Er ions at liquid nitrogen temperature in order to introduce a desirable concentration of Er and (ii) Ge ions to high doses at higher temperatures in order to induce a spontaneous formation of a nanoporous structure whose ligaments are uniformly doped with Er.

<sup>10</sup>L. R. Doolittle, *Nucl. Instrum. Methods Phys. Res. B* **9**, 344 (1985).

<sup>11</sup>L. Csepregi, R. P. Kuellen, J. W. Mayer, and T. W. Sigmon, *Solid State Commun.* **21**, 1019 (1977); C. J. Palmstrom and G. J. Galvin, *Appl. Phys. Lett.* **47**, 815 (1985); A. Satta, E. Simoen, T. Clarysse, T. Janssens, A. Benedetti, B. De Jaeger, M. Meuris, and W. Vandervorst, *ibid.* **87**, 172109 (2005).

<sup>12</sup>Note that the sample annealed at 800 °C [Fig. 2(c)] was prepared conventionally, by mechanical grinding followed by thinning in an ion-polishing system, while the dark contrast visible above the Ge sample surface in bright-field XTEM images in Figs. 2(a) and 2(b) is due to a protective Pt layer deposited on the sample surfaces before the cross sections were extracted in a dual-beam focused ion beam (FIB) instrument. We also note that Ge surface amorphization is expected during the initial stages of the ion-beam-assisted deposition of such a protective Pt layer (with 30 keV Ga ions at room temperature) in the FIB. However, the facts that (i) Er precipitation is clearly observed at the *a/c* interface in Figs. 2(a) and 2(b) and (ii) the thicknesses of the surface amorphous layers measured by RBS/C and XTEM are comparable strongly suggest that these surface amorphous layers are not an artifact of FIB sample preparation process.

<sup>13</sup>Note that, for bombardment with 110 keV ErO cluster ions, the depth profiles of Er and O atoms have a significant overlap since the heavier Er atom carries most of the kinetic energy (100.3 keV) of the 110 keV ErO cluster. Indeed, calculations with the TRIM code (Ref. 14) show that the projected ranges of 100.3 keV Er and 9.7 keV O ions in Ge are 286 and 210 Å, respectively.

<sup>14</sup>J. F. Ziegler, J. P. Biersack, and U. Littmark, *The Stopping and Range of Ions in Solids* (Pergamon, New York, 1985), 1, 109.

<sup>15</sup>V. Touboltsev and P. Jalkanen, *J. Appl. Phys.* **97**, 013526 (2005), and references therein.

<sup>16</sup>See, for example, G. L. Olson and J. A. Roth, *Mater. Sci. Rep.* **3**, 1 (1988); R. G. Elliman and Z. W. Fang, *J. Appl. Phys.* **73**, 3313 (1993); H. Francois-Sait-Cyr, E. Anoshkina, F. Stevie, L. Chow, K. Richardson, and D. Zhou, *J. Vac. Sci. Technol. B* **19**, 1769 (2001); P. Zhang, F. Stevie, R. Vanfleet, R. Neelakantan, M. Klimov, D. Zhou, and L. Chow, *J. Appl. Phys.* **96**, 1053 (2004).

<sup>17</sup>M. J. Aziz, J. T. Tsao, M. O. Thompson, P. S. Peercy, and C. W. White, *Phys. Rev. Lett.* **56**, 2489 (1986).

<sup>18</sup>K. A. Jackson, K. M. Beatty, and K. A. Gudgel, *J. Cryst. Growth* **271**, 481 (2004).

<sup>19</sup>Additional studies are currently needed to ascertain if Er precipitation can be avoided when annealing temperatures  $< 400\text{ }^{\circ}\text{C}$  are used and whether the amorphous phase recrystallization and Er segregation processes are different in bulk Ge, studied here, and Ge nanostructures.